



Communication

Advancing Ultra-High Precision in Satellite–Ground Time–Frequency Comparison: Ground-Based Experiment and Simulation Verification for the China Space Station

Yanming Guo ^{1,2,†} , Shuaihe Gao ^{1,*,†}, Zhibing Pan ^{1,†}, Pei Wang ¹, Xuewen Gong ¹, Jiangyu Chen ³, Kun Song ³, Zhen Zhong ³, Yaoli Yue ⁴, Lishu Guo ¹, Yan Bai ¹, Yuping Gao ¹, Xiaochun Lu ^{1,2} and Shougang Zhang ^{1,2}

- ¹ National Time Service Center, Chinese Academy of Sciences, Xi'an 710600, China; guoyanming@ntsc.ac.cn (Y.G.); panzhibing@ntsc.ac.cn (Z.P.); wangpei@ntsc.ac.cn (P.W.); gongxuewen@ntsc.ac.cn (X.G.); guolishu@ntsc.ac.cn (L.G.); by@ntsc.ac.cn (Y.B.); gaoyup@ntsc.ac.cn (Y.G.); luxc@ntsc.ac.cn (X.L.); szhang@ntsc.ac.cn (S.Z.)
- ² University of Chinese Academy of Sciences, Beijing 100039, China
- ³ The 29th Research Institute of China Electronics Technology Group Corporation, Chengdu 611731, China; chjiangy@sina.com (J.C.); songkun1122@foxmail.com (K.S.); 15608172230@163.com (Z.Z.)
- ⁴ The 34th Research Institute of China Electronics Technology Group Corporation, Guilin 541010, China; 13635199784@163.com
- * Correspondence: gaoshuaihe@ntsc.ac.cn
- † These authors contributed equally to this work.

Abstract: Establishing an ultra-high-precision link for time–frequency comparisons between satellites and ground stations is critically important. This endeavor is fundamental to the advancement of pioneering space science exploration and the development of a robust space-based time–frequency system featuring ultra-high-precision space atomic clocks. In response to the requirements for assessing the long-term stability of high-precision space atomic clocks, we have designed and implemented a satellite–ground microwave time–frequency comparison system and method based on a three-frequency mode. Ground-based experimental results demonstrate that the equipment layer can achieve a satellite–ground time comparison accuracy better than 0.4 ps (RMS), with the equipment delay stability (ADEV) for all three frequencies being better than 8×10^{-18} at 86,400. By leveraging the ground-based experimental results, we constructed a satellite–ground time–frequency comparison simulation and verification platform. This platform realizes ultra-high-precision satellite–ground time–frequency comparison based on the China Space Station (CSS). After correcting various transmission delay errors, the satellite–ground time comparison achieved an accuracy better than 0.8 ps and an ADEV better than 2×10^{-17} at 86,400. This validation of our novel satellite–ground time–frequency comparison system and method, capable of achieving an 10^{-17} magnitude stability, is not only a significant contribution to the field of space time–frequency systems but also paves the way for future advancements and applications in space science exploration.

Keywords: satellite–ground microwave time–frequency comparison; three-frequency mode; China Space Station (CSS); transmission delay errors; stability



Citation: Guo, Y.; Gao, S.; Pan, Z.; Wang, P.; Gong, X.; Chen, J.; Song, K.; Zhong, Z.; Yue, Y.; Guo, L.; et al. Advancing Ultra-High Precision in Satellite–Ground Time–Frequency Comparison: Ground-Based Experiment and Simulation Verification for the China Space Station. *Remote Sens.* **2023**, *15*, 5393. <https://doi.org/10.3390/rs15225393>

Academic Editor: Michael E. Gorbunov

Received: 19 October 2023
Revised: 8 November 2023
Accepted: 14 November 2023
Published: 17 November 2023



Copyright: © 2023 by the authors. Licensee MDPI, Basel, Switzerland. This article is an open access article distributed under the terms and conditions of the Creative Commons Attribution (CC BY) license (<https://creativecommons.org/licenses/by/4.0/>).

1. Introduction

Globally, the development of high-precision space atomic clocks is regarded as a vital direction in the exploration of cutting-edge space science. These sophisticated timekeepers are capable not only of maintaining precise time on Earth but also of facilitating precise time–frequency comparisons at any location in space, which is particularly crucial for fundamental physics research. The capability for spatial time–frequency comparison enables the detection of spacetime variations in different gravitational fields, playing a pivotal role in advanced fundamental physical research such as the measurement of gravitational redshift and the determination of the fine-structure constant. Current GNSS

systems such as BDS, Galileo, and GPS III achieve 10^{-14} to 10^{-15} stability at one day while offering enhanced time and frequency transfer via commercial services, while the Two-Way Satellite Time and Frequency Transfer (TWSTFT) method employs two-way satellite signals to compare terrestrial clocks, achieving stability of the order of 10^{-15} by leveraging the symmetry of the two-way transmission to enhance measurement stability. Led by the European Space Agency, the European Advanced Atomic Clock Program (Atomic Clock Ensemble in Space, ACES) plans to equip the International Space Station (ISS) with a combination of cold atomic microwave clocks and active hydrogen maser clocks, and the ACES MWL system is aimed at achieving a satellite–ground comparison capability with an uncertainty and daily stability reaching the 10^{-16} level. Furthermore, this will pave the way for advanced experiments in cold atomic physics and relativity tests [1]. In comparison with the ACES initiative, the high-precision time–frequency scientific experiment system of the China Space Station (CSS) intends to deploy and operate an ultra-high-precision atomic clock combination, including cold atomic strontium optical clocks, cold atomic microwave clocks, and active hydrogen maser clocks. Simultaneously, by leveraging both microwave and laser transmission links, the CSS aspires to achieve ultra-high-precision comparisons between space- and ground-based clocks, enhancing long-term stability [2]. Additionally, the European Space Agency has laid out its plans for the development of space optical clocks (SOC). In the project’s second phase, they have realized a space optical clock prototype with a long-term stability of 5×10^{-17} . Plans are in place to install this on the ISS [3]. Hence, establishing a high-precision satellite–ground time–frequency comparison link, objectively assessing the performance of space atomic clock groups, and promoting the application of high-precision time–frequency references are important research directions.

In the realm of scientific experimentation, optical techniques, including frequency combs and continuous-wave lasers, have shown remarkable progress, and measurement techniques based on free-space optical frequency comb signal comparisons have garnered significant attention and development [4–7], with early systems achieving 10^{-16} instability in one second and recent advancements pushing this to 3×10^{-18} [8]. Dual-branch comb designs have yielded Allan deviations of approximately 2×10^{-18} over one second and an ultimate stability of approximately 5×10^{-21} over 100,000 s after noise reduction [9]. Although lab-based free-space optical frequency comb techniques have shown high accuracy, their performance is greatly diminished in atmospheric conditions, making long-distance clock comparisons challenging. Therefore, the laser satellite–ground time–frequency transmission, implemented using the optical frequency comb, inherently exhibits vulnerabilities. It is severely disrupted by atmospheric conditions that compromise its continuous operational capability. Moreover, because of the high-speed relative motion between satellites and the Earth, the simplistic relativistic correction models currently in use substantially limit the precision of correcting time delay errors caused by relative positional changes of satellite payloads [10]. Consequently, the application of lasers to achieve space optical frequency comb signal comparisons in the complex satellite–ground environment may be constrained. There is the potential that it might not meet the demands for ultra-high precision in satellite–ground time–frequency comparisons. This underscores the importance of improving microwave time–frequency comparison methods, which may better withstand atmospheric disturbances and maintain a stable long-term space–ground link. Advancements in microwave time–frequency comparison methods may hold the key to realizing a future global network of ultra-high-precision clock comparisons.

In response to the requirements for evaluating the long-term stability of satellite–ground time–frequency in the high-precision time–frequency experimental system of the China Space Station (CSS), this paper focuses on the microwave time–frequency transmission payload planned to be on board the space station. In collaboration with a ground station (GS) system, we have constructed a simulated satellite–ground time–frequency comparison system. Utilizing this system, we validated the design of a terrestrial three-frequency mode (1 uplink + 2 downlink) for time–frequency comparisons. Through system architecture, error modeling and correction, and equipment control, we demonstrate the

feasibility of achieving ps-level satellite–ground time–frequency comparison. Additionally, we show that long-term continuous operation can attain stability of the order of 10^{-17} for satellite–ground time–frequency comparison.

2. Satellite (CSS)–Ground Time–Frequency Comparison System and Methodology

The CSS is equipped with an array of time–frequency payload equipment, which includes advanced onboard atomic clocks—such as a hydrogen maser, a microwave clock, and an optical clock—integral for maintaining the station’s time standards with ultra-high precision. Alongside these clocks, the CSS hosts external payloads like the microwave link [11] payload, laser link payload, and precise orbit determination antenna payload. These payloads, in combination with the ground station equipment, form a comprehensive satellite–ground time–frequency comparison system [12]. This system, as depicted in Figure 1, is designed to facilitate ultra-high-precision time–frequency comparisons between the satellite and ground, enabling critical operations and experiments that require stringent time synchronization and frequency standards.

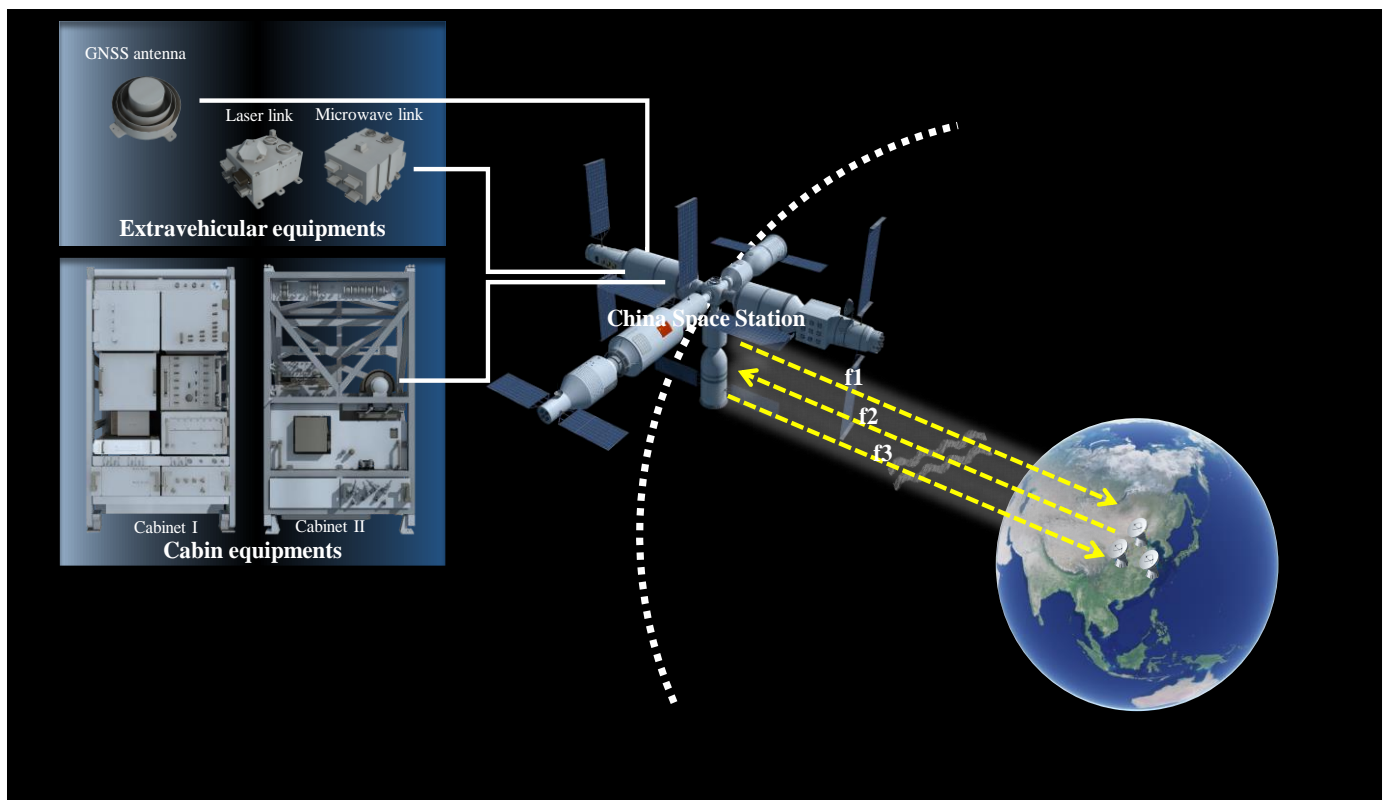


Figure 1. Satellite (CSS)–Ground Time–Frequency Comparison System.

In response to the stability assessment requirements of the high-precision time–frequency system on the CSS, a three-frequency mode has been designed for satellite–ground time–frequency comparison based on the aforementioned comparison system. When taking into full consideration the signal path effects, the three-frequency mode (1 uplink + 2 downlinks) of the satellite–ground microwave two-way link is expected to achieve ultra-high precision in satellite–ground time–frequency comparison. The uplink and downlink (f_1 and f_2) are used to decouple satellite–ground relative clock differences, while the two downlinks (f_1 and f_3) are for atmospheric error modeling. The observation model for this three-frequency-mode satellite–ground time–frequency comparison can be represented as

$$\begin{cases} p_1(t, f_1) = r_G^S(t) + \Delta T(t) + H_G^S(f_1) + \tau_{ion}(t, f_1) + \tau_{tro}(t, f_1) + \tau_{mov}(t, f_1) + \tau_{rel}(t, f_1) + \varepsilon_G^S(t, f_1) \\ p_2(t, f_2) = r_S^G(t) - \Delta T(t) + H_S^G(f_2) + \tau_{ion}(t, f_2) + \tau_{tro}(t, f_2) + \tau_{mov}(t, f_2) + \tau_{rel}(t, f_2) + \varepsilon_S^G(t, f_2) \\ p_3(t, f_3) = r_S^G(t) - \Delta T(t) + H_S^G(f_3) + \tau_{ion}(t, f_3) + \tau_{tro}(t, f_3) + \tau_{mov}(t, f_3) + \tau_{rel}(t, f_3) + \varepsilon_S^G(t, f_3) \end{cases} \quad (1)$$

where $f_1 \sim 25$ GHz, $f_2 \sim 30$ GHz, and $f_3 \sim 20$ GHz represent one uplink signal frequency and two downlink signal frequencies, respectively. The variable p stands for the carrier observation value at different frequency points, while r signifies the geometric distance equivalent time delay between satellite and ground receivers at different moments, and $\Delta T(t)$ is the relative clock offset between satellite and ground at different times. H_G^S is the sum of the ground equipment transmission channel delay and the space equipment reception channel delay. Conversely, H_S^G is the combined delay of the space equipment transmission channel and the ground equipment reception channel. The variables τ_{ion} , τ_{tro} , τ_{mov} and τ_{rel} represent the equivalent time delays for ionospheric error, tropospheric error, movement error, and relativistic effects, respectively. While some error factors are fundamentally independent of frequency, frequency is related to the signal path that is affected by frequency. In our work, frequency serves to differentiate the error factors along distinct signal paths, thus reflecting the indirect relationship between the two. ε denotes measurement error.

In two-way time–frequency transmission under satellite–ground conditions, the uplink and downlink propagation signals have an approximate symmetry in their paths. By leveraging the difference in ranging values from the uplink and downlink two-way links, we can decouple the relative clock difference between satellite and ground. Most of the transmission errors introduced by the propagation path can be either canceled out or significantly attenuated. The decoupled relative clock difference between the satellite and the ground is given by

$$\Delta T(t) = \frac{p_1(t, f_1) - p_2(t, f_2)}{2} + \Delta H_{hardware}^{f_1, f_2} + \Delta \varepsilon_{obs}^{f_1, f_2} + \Delta \tau_{ion}^{f_1, f_2} + \Delta \tau_{tro}^{f_1, f_2} + \Delta \tau_{mov}^{f_1, f_2} + \Delta \tau_{rel}^{f_1, f_2} \quad (2)$$

where p_1 and p_2 represent the ranging values of the uplink and downlink, respectively, typically obtained through transceiver devices that mutually exchange carrier waves and pseudocode ranging signals. $\Delta H_{hardware}$ denotes the combined delay error intrinsic to the hardware, usually determined via a self-closed loop calibration. $\Delta \tau_{ion}$, $\Delta \tau_{tro}$, $\Delta \tau_{mov}$ and $\Delta \tau_{rel}$ signify transmission errors along the link, corresponding respectively to ionospheric, tropospheric, motion time delay, and relativistic errors, typically estimated through precise modeling. $\Delta \varepsilon_{obs}$ is the measurement error, predominantly determined by the inherent hardware capabilities of the transmitting and receiving devices.

The precision of equipment measurement errors is the most pivotal factor in determining the accuracy of satellite–ground time delay measurements. Apart from the errors in measurement equipment, other error sources such as platform orbiting accuracy and atmospheric transmission conditions also affect the final two-way time comparison results [13]. Hence, the correction of transmission delay errors for distance measurement signals is vital for achieving high-precision two-way time comparisons. Strategies and methods for modeling various types of errors are shown in Table 1.

Table 1. Satellite–ground transmission delay errors and correction methods.

| Error | Error-Handling Method |
|--|--|
| Time delay caused by motion | Corrected by model [14] |
| Hardware delay | Closed-loop self-calibration [15] |
| Time delay caused by troposphere effect | Using microwave radiometer data and model [16] |
| Time delay caused by ionosphere effect | Corrected by dual-downlink model [16] |
| Time delay caused by relativistic effect | Corrected by model [17] |

Assuming the hardware capabilities meet the required standards, to attain an ultra-high time-transfer link accuracy, it is imperative to thoroughly consider the mentioned error sources and adopt appropriate methods to precisely counteract these errors to ensure the stability of the link.

3. Ground-Based Experiment

In high-precision link systems, the inherent measurement errors of the equipment significantly determine its measurement accuracy. To assess the intrinsic metrics of the link equipment developed for measurements, a co-source test scenario is contemplated. This involves using a single time–frequency reference signal for both the satellite-borne and ground-based terminals, thus eliminating errors introduced by the clock group and assessing the additional noise of the microwave time–frequency transfer link. A ground-based bidirectional test system is established as shown in Figure 1, simulating both the space and ground segments. The GNSS receiver is employed to initialize the pulse-per-second synchronization between the space and ground segments, assisting in the rapid establishment of the satellite–ground link. Subsequently, the local optical-frequency reference signal maintains the pulse moments for both the satellite-borne and ground-based terminals.

The test system utilizes optical-frequency signal transmission to achieve precise time-delay control and local oscillator signal synthesis, as shown in the equipment composition in Figure 2. The frequency signal from the cesium atomic clock is converted to an optical signal via an optical comb. Using an optical-frequency-signal phase-stable transmission device, precise time-delay control is achieved during the optical-frequency signal transmission process. Pulse repetition frequency multiplication is implemented at the optical frequency, which, after photodetection, filtering, and amplification, is converted into the desired local oscillator signal. Stable tracking and precise measurement are realized through radio frequency conversion and baseband signal processing. Furthermore, for the assurance of the test equipment’s long-term stability, the experimental setup incorporates comprehensive thermal regulation measures: externally, it utilizes protective radomes and precision air conditioning to manage the ambient temperature, while internally, a secondary precision temperature control system, consisting of liquid cooling pipelines, heating films, and thermoelectric coolers (TECs), meticulously maintains the equipment’s thermal state.

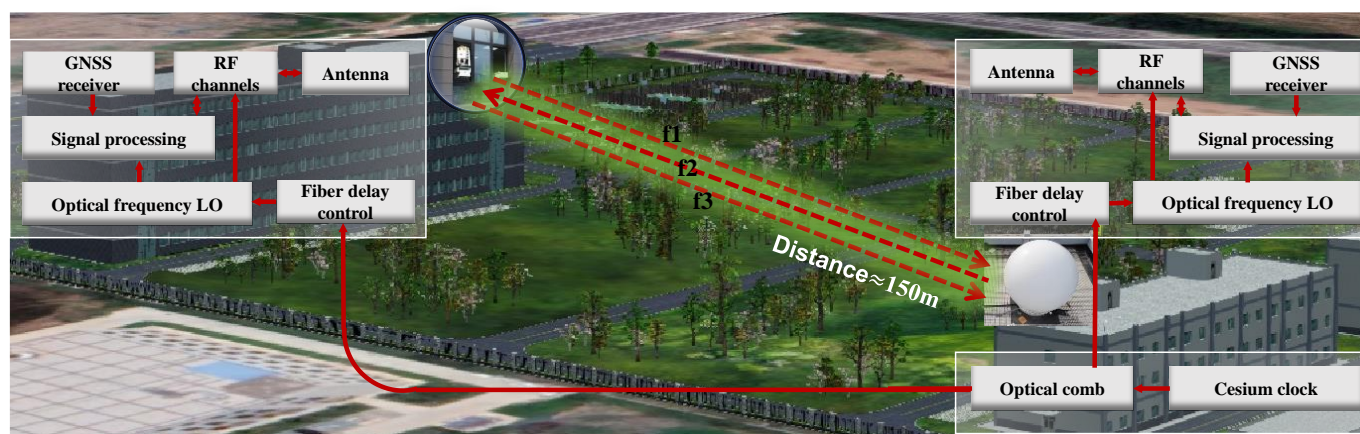


Figure 2. Ground-Based Test Experiment Setup.

The measurement accuracy at the equipment level is a critical factor constraining the high-precision time–frequency comparison between the satellite and the ground. This primarily includes random measurement errors of the equipment, equipment time delay caused by temperature changes, and jitter in the antenna phase center, among others. Based on the aforementioned ground test system, measurements obtained from satellite-borne and ground-based transceiver equipment in terrestrial conditions showed time delay measurement results for the transmission links at three frequency points. Figure 3 and Table 2

display the one-way time delay measurement results for two uplinks and one downlink in a co-source test scenario. The time deviation (TDEV) values for the three frequency points were found to be 3.72×10^{-3} ps at 86,400 s, 6.50×10^{-2} ps at 86,400 s, and 1.32×10^{-1} ps at 86,400 s, respectively. The root mean square (RMS) values of their link measurement errors are all less than 0.4 ps. The corresponding Allan deviation (ADEV) values were 5.84×10^{-19} at 86,400 s, 2.27×10^{-18} at 86,400 s, and 7.65×10^{-18} at 86,400s, respectively. This shows that the ground-based experiment for the three-frequency microwave transfer link in near space has high stability, indicating that the currently designed time delay measurement system possesses the fundamental hardware capability of achieving satellite-ground time-frequency comparisons at the 10^{-17} level. This represents nearly a 3-order-of-magnitude improvement over the precision of the BDS-3 satellite-ground time comparison system [18,19].

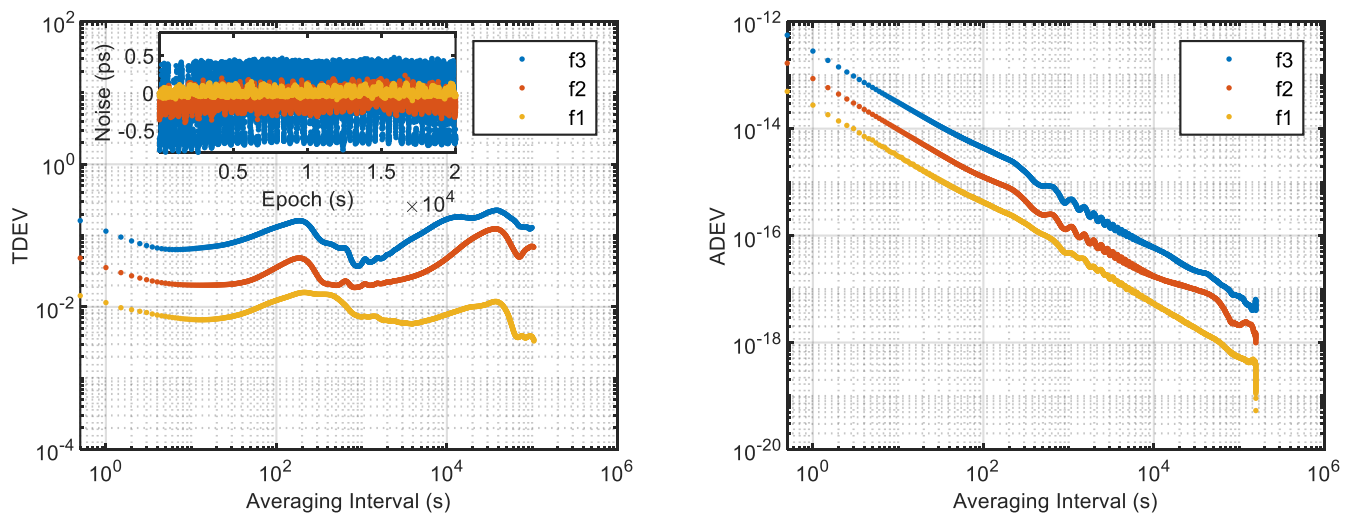


Figure 3. Experimental results of ground time–frequency transfer. Left: The TDEV (ps) of three–frequency links. Right: The ADEV of three–frequency links.

Table 2. Statistics on stability of three–frequency links.

| Type | Averaging Interval | CSS Receiving Link (f1) | GS Receiving Link (f2) | GS Receiving Link (f3) |
|------|--------------------|-------------------------|------------------------|------------------------|
| TDEV | 300 s | 1.50×10^{-14} | 4.05×10^{-14} | 9.76×10^{-14} |
| | 86,400 s | 3.72×10^{-14} | 6.50×10^{-14} | 1.32×10^{-13} |
| ADEV | 300 s | 1.74×10^{-16} | 4.73×10^{-16} | 1.62×10^{-15} |
| | 86,400 s | 5.84×10^{-19} | 2.27×10^{-18} | 7.65×10^{-18} |

4. Simulation and Verification of Satellite–Ground Time–Frequency Comparison

In conditions where satellite and ground equipment have functional states, the primary limiting factor of the accuracy of satellite–ground time–frequency comparison is the correction of transmission delay errors. The design of a three-frequency satellite–ground time–frequency comparison system requires modeling and correcting transmission delay errors item by item. Therefore, the orbital products and microwave radiometer monitoring parameters (pressure P , temperature T , water vapor pressure e_w) used for correction are key factors influencing correction accuracy. Among them, the accuracy of orbital products is affected by three factors: errors in precise orbit determination (POD), spacecraft attitude errors, and calibration errors in the conversion process from the tracking antenna phase center to the microwave antenna phase center. Meanwhile, the primary cause of errors in atmospheric parameter monitoring values by microwave radiometers is instrument error. According to current actual ground test results, the aforementioned error factors can generally be controlled within the index range listed in Table 3. Therefore, the simulation and

analysis of satellite–ground time–frequency comparison are based on the index capabilities listed in the table.

Table 3. Error indicator settings.

| | |
|--------------------------------|---|
| Attitude error | $\leq 40''$ (3σ) |
| Phase center calibration error | ≤ 3 mm (3σ) |
| POD error | ≤ 10 cm (3σ) |
| Atmospheric parameter error | $P \leq 0.5$ hPa; $T \leq 0.5$ °C; $e_w \leq 0.5$ hPa |

4.1. Satellite–Ground Simulation and Verification Platform

In order to simulate and validate the satellite–ground time–frequency comparison system and its related key technologies, this paper constructs a satellite–ground time–frequency simulation and verification platform. The construction is based on the CSS orbital parameters provided by the China Manned Space Agency office (<http://www.cmse.gov.cn/gfgg/zgkjzgdcs/> accessed on 16 July 2023) as shown in Table 4, as well as related parameters obtained from ground-based experiments. Utilizing this simulation platform, we conducted satellite–ground simulations to validate ultra-high-precision satellite–ground microwave time–frequency comparison technology. The architecture of the simulation and verification platform is illustrated in Figure 4.

Table 4. CSS orbital configurations.

| Epoch | 24 February 2022 00:00:00 (UTC) |
|--------------------|---|
| Orbital parameters | Semi-major axis: 6759.9132 m, Orbit inclination: 41.4680 (degree) Eccentricity: 0.0005007, Right ascension of ascending node: 188.6126 (degree) Argument of perigee: 357.7510 (degree), Mean anomaly: 1.8149 (degree) |

Within the framework of the simulation and verification platform, parameters are strictly set according to the actual conditions of the CSS [20]. In this simulation, we have comprehensively considered the Earth’s model and the forces acting on the spacecraft and modeled various error factors, including geometric distance, motion time delay (distance error and clock error), atmospheric time delay, and relativistic time delay, among others [13]. This process almost accurately replicates the entire procedure of the satellite–ground time–frequency comparison system achieving two-way measurement. The simulation generates dual one-way pseudo-range observation data between the CSS and the ground (with a sampling rate of 1 Hz). Lastly, according to the simulation data, we further analyze the impact of various error factors under this new method of satellite–ground time comparison. We also validate the feasibility of achieving time stability for the satellite–ground comparison, thereby providing technical support for the processing and analysis of subsequent in-orbit experimental data.

4.2. Analysis of Transmission Delay Errors in Satellite–Ground Time–Frequency Comparison

Utilizing the CSS-to-ground simulation, we replicated the establishment of a CSS-to-ground measurement link over the course of a single day (0~86,400 s) under realistic environmental conditions. This simulation provided us with a detailed understanding of various two-way transmission delay errors in the satellite–ground comparison. As illustrated in Figure 5, each arc represents one of the successive passes of the CSS, indicating the periods when the space station is visible from a ground observer’s perspective. Typically, these visibility arcs last for approximately 4 to 6 min, a time frame that is critical for the successful establishment and maintenance of a measurement link between the CSS and ground station.

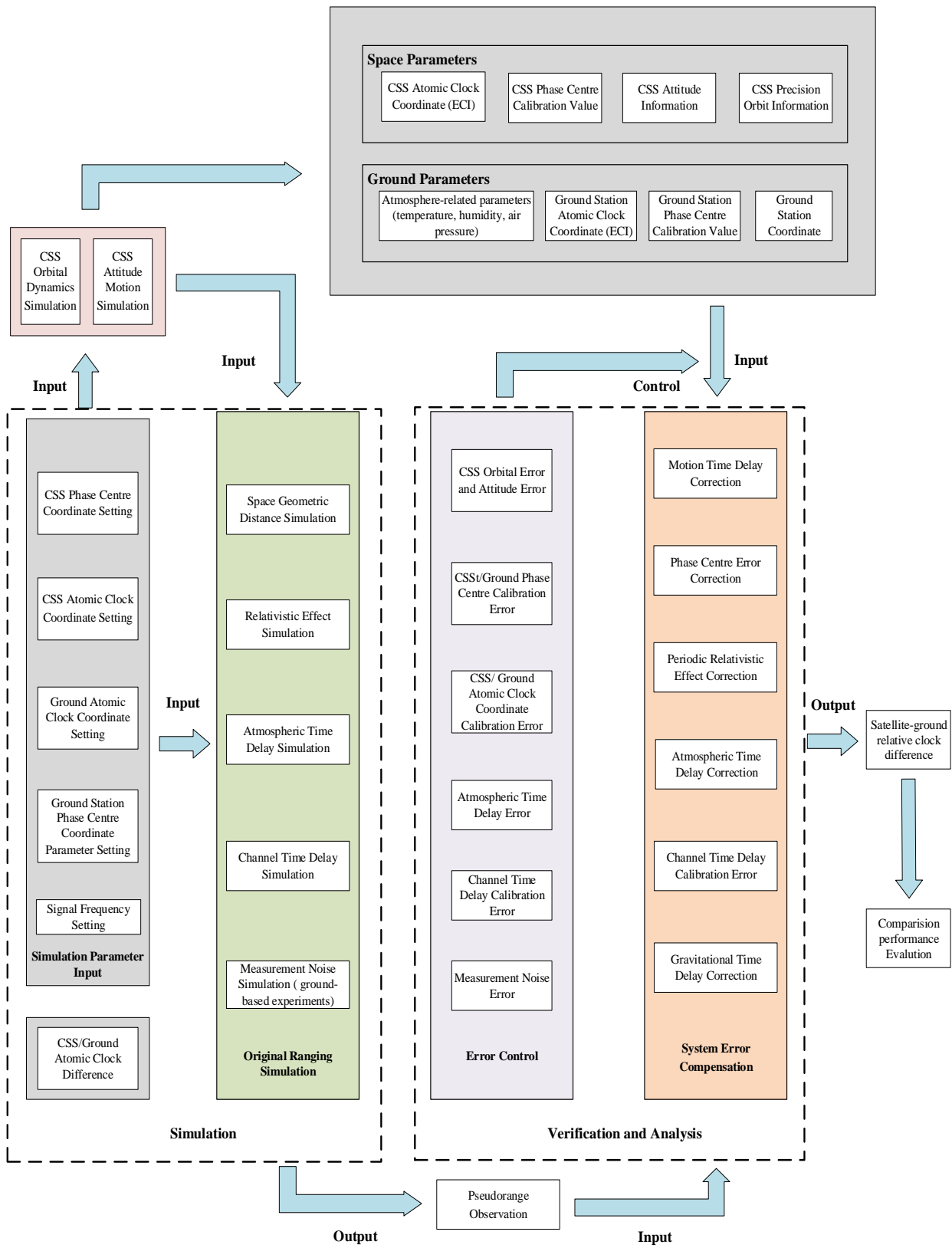


Figure 4. Platform architecture of the satellite-ground simulation and verification.

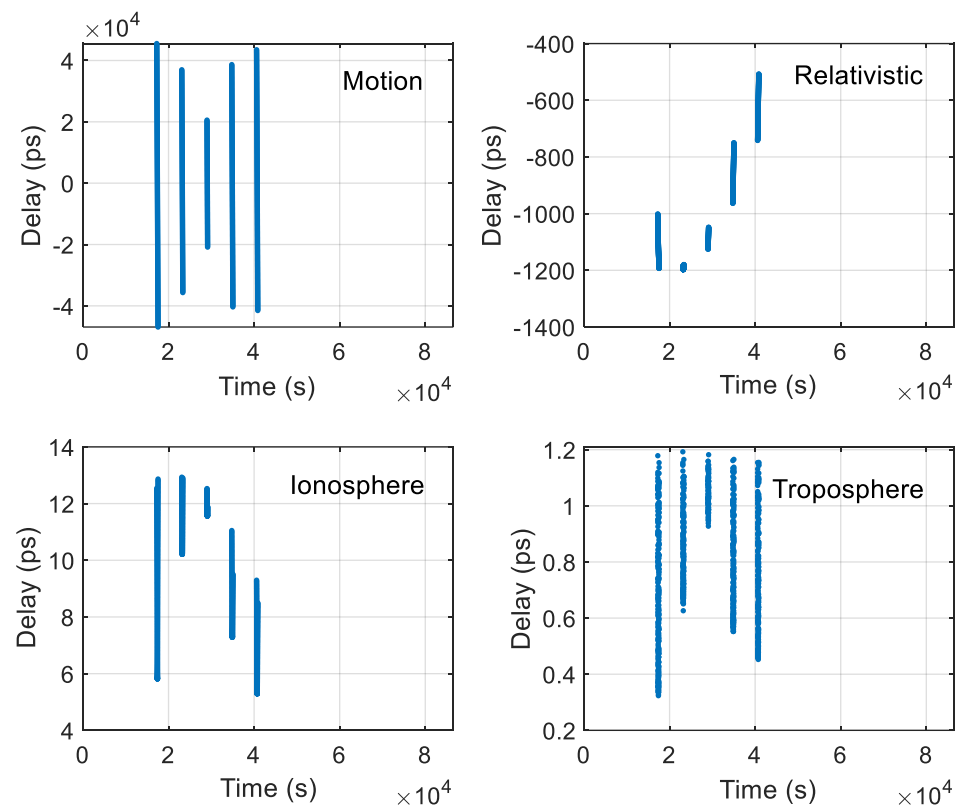


Figure 5. Two-way transmission delay errors of satellite-ground comparison.

In Figure 5, the x-axis represents time within the day in seconds, outlining the evolution of two-way time delays throughout the link establishment between the space station and the ground station. These delays encompass motion-induced delay, relativistic effects, and atmospheric interferences such as ionospheric and tropospheric delays, which align with the error terms outlined in Equation (2). Each data point plotted signifies a separate simulation instance, reflecting the variation in time delays across different runs. Because of the low Earth orbit and high velocity of the space station, the motion delay error introduced during signal transmission significantly impacts the satellite-ground time comparison. As shown, the error can accumulate to tens of nanoseconds in the process of the two-way decoupling of clock differences, thereby underscoring the necessity of correcting for the motion delay error. This is typically achieved through the use of precise ephemeris data for correction. Our simulations indicate that when applying precise ephemeris modeling to correct for motion delay error on low-Earth-orbit spacecraft, the residual uncertainty in the error can be reduced to better than picoseconds.

According to the theory of relativity, the simultaneity of spatially separated events is not absolute. In satellite-ground time-frequency comparison, relativistic errors mainly arise from the high-speed relative motion between the targets. This includes the effects of relativity on frequency (nominal frequency offset and periodic relativistic time delay) and relativistic path effects (Shapiro time delay). The nominal frequency offset caused by relativity can be precisely calibrated by lowering the frequency of the atomic clocks on the spacecraft or ground station, and it is generally insufficient to affect the stability of long-distance time comparisons. The periodic relativistic effects during the space-station-to-ground time comparison are mainly due to the different speeds and gravitational potentials of the atomic clocks on the space station and ground station in inertial space. In low Earth orbit, the spacecraft is subject to complex forces, and the gravitational potential modeling must consider various perturbing forces (mainly, Earth's gravity, tides, lunar and solar gravity, and solar radiation pressure). Gravitational time delay is caused by changes in the relative positions of the ground station, spacecraft, and Earth's center during the

propagation of the satellite–ground ranging signal. As shown in Figure 5, in the high-precision time–frequency comparison experiment system of the CSS, the time-delay errors caused by relativity reached several nanoseconds. To achieve accurate estimation and correction of this part of the error, we consider establishing a high-precision model for the forces acting on the space station to mitigate the impact of periodic relativistic time-delay perturbations on time comparison stability.

Atmospheric errors (ionosphere and troposphere) during signal propagation also significantly limit the achievement of ultra-high-precision microwave satellite–ground time comparison. In the process of the bi-directional decoupling of clock differences in three-frequency mode, the error can reach tens of picoseconds, which requires careful consideration and correction. To address atmospheric errors, we propose a novel approach that eliminates tropospheric errors by modeling historical data and microwave radiometer monitoring data. In combination with two downlink links, we accurately calculate the total electron content of the ionosphere along the same path, thereby correcting the time delay errors caused by the ionosphere. Utilizing the current design of high-precision error-correction methods (see Table 1), we corrected various link delay errors in the three-frequency mode. The residual errors of the two-way time–frequency comparison after correction are illustrated in Figure 6. After correction, the RMS of the residual error of the satellite–ground two-way transmission delay errors is no more than 0.8 ps. The corresponding TDEV can achieve daily stability better than 1.33×10^{-3} ps, and ADEV can achieve daily stability better than 1.50×10^{-17} . It is evident that even after two-way differencing and correction, the transmission delay errors still have significant impacts on the stability of the satellite–ground time comparison compared to the equipment delay stability (Table 2). This makes transmission delay errors one of the main factors affecting the stability of time–frequency comparison [21]. The handling of transmission delay errors directly affects the final results of satellite–ground time comparison.

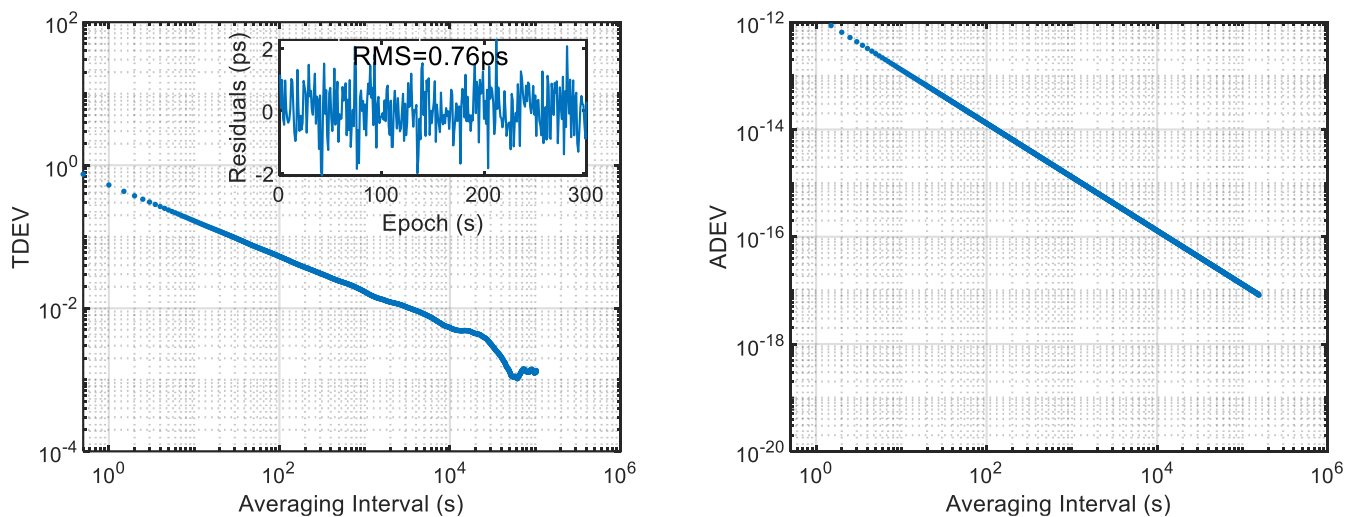


Figure 6. Stability of the residual error after correcting various transmission–delay errors in two–way time–frequency comparison.

4.3. Analysis of Satellite–Ground Time–Frequency Comparison Results

Based on the current ground experiments, and taking into account the various error factors in satellite–ground comparison as mentioned above, a semi-physical satellite–ground time comparison processing platform has been established. The satellite–ground time comparison results in the three-frequency mode are shown in Figure 7. With the help of the ultra-high–precision atomic clock on board the space station, we expect to achieve a satellite–ground time comparison precision of 0.77 ps. The corresponding TDEV can achieve 2.94×10^{-2} ps at 86,400 s, and ADEV can achieve 1.51×10^{-17} at 86,400. Therefore, considering this satellite–ground time–frequency comparison system, it is ex-

pected to achieve an 10^{-17} magnitude of stability in the CSS–ground time–frequency comparison system.

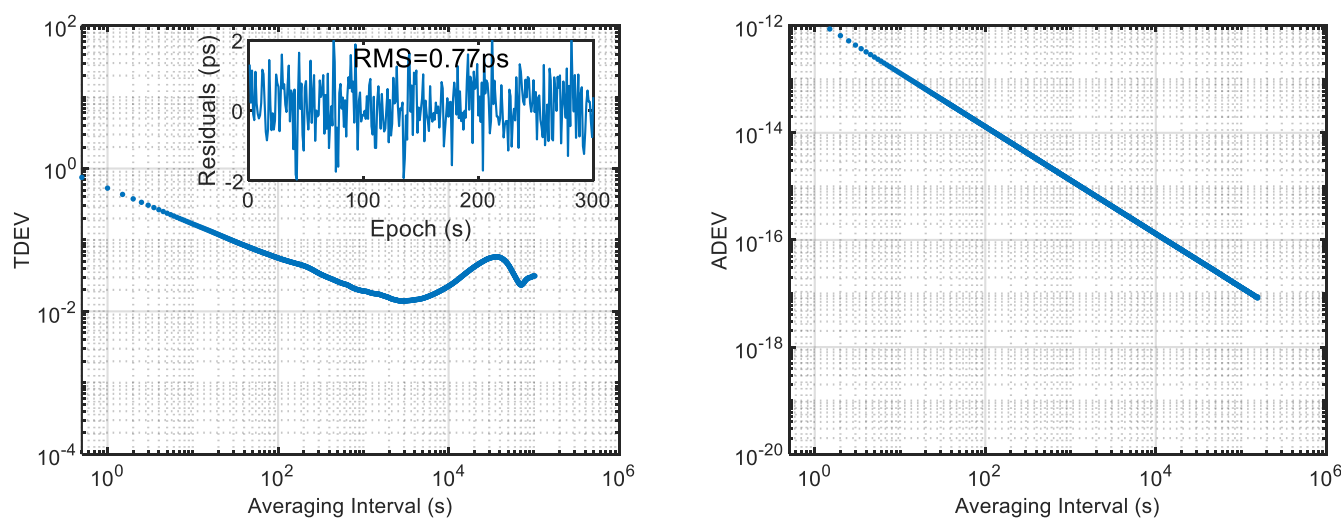


Figure 7. Final stability of the satellite (CSS)–ground time comparison.

5. Conclusions and Future Work

In response to the need for long-term stability assessment of satellite–ground time–frequency comparison in the CSS, this paper proposes a three-frequency-mode satellite–ground time difference measurement system and method. According to ground experiment results, the equipment is capable of achieving a measurement error with the RMS of less than 0.4 ps, as well as stability better than 8×10^{-18} at 86,400 s. Taking into account the impact of transmission delay errors and other factors (including link residual errors, hardware measurement inaccuracies, and clock noise, effectively reflecting the total uncertainty in our measurements), our comprehensive analysis and evaluation indicate that the precision of satellite–ground time comparison is expected to be better than 0.8 ps, meeting the requirements of 10^{-17} magnitude stability for satellite–ground time–frequency comparison.

Our initial use of different frequencies was a strategic choice to maintain signal integrity while developing these isolation techniques. To further enhance the precision of satellite–ground time–frequency comparison, future work will focus not only on refining corrections for atmospheric and relativistic errors but also on addressing the technical challenges associated with same-frequency uplink and downlink. We plan to optimize the system and scheme design for same-frequency communications, by implementing effective isolation measures to mitigate the potential interference of signals in space. This approach is aimed at ensuring the symmetry of the propagation paths for uplink and downlink signals, which is expected to inherently cancel out the effects of the space environment on the signals. At the same time, we will consider the impact of higher-order perturbing forces in the inertial frame (such as J2 terms and above) on the precision of two-way time comparison. We aim to establish a precision relativistic correction model based on higher-order terms to correct the satellite–ground time comparison errors caused by signal propagation, thereby achieving higher precision in satellite–ground time comparison.

Author Contributions: Conceptualization, Y.G. (Yanming Guo) and Z.P.; data curation, Y.G. (Yanming Guo); formal analysis, Y.G. (Yanming Guo) and X.G.; funding acquisition, S.G., Y.B., Y.G. (Yuping Gao), X.L. and S.Z.; methodology, Y.G. (Yanming Guo); project administration, Y.G. (Yanming Guo), S.G. and Z.P.; resources, J.C., K.S., Z.Z., Y.Y. and L.G.; validation, Y.G. (Yanming Guo), Z.P. and X.G.; writing—original draft, Y.G. (Yanming Guo) and P.W.; writing—review and editing, Y.G. (Yanming Guo) and Z.P. All authors have read and agreed to the published version of the manuscript.

Funding: This research was supported by the National Natural Science Foundation of China (12273045, 42030105).

Data Availability Statement: The simulation data supporting the findings of this study are available upon request from the authors. These data are not publicly available due to privacy or ethical restrictions. For specific inquiries regarding the data, please contact the corresponding author.

Conflicts of Interest: The authors declare no conflict of interest.

References

1. Laurent, P.; Abgrall, M.; Clairon, A.; Lemonde, P.; Santarelli, G.; Salomon, C.; Picard, F.; Sirmain, C.; Massonnet, D.; Cacciapuoti, L. The space program PHARAO/ACES. *Proc. Spie* **2007**, *6673*, 50–62.
2. Liu, Y. *Study on Space Station and Loran Common-View Time Comparison Method*; University of Chinese Academy of Sciences: Beijing, China, 2019.
3. Origlia, S.; Pramod, M.S.; Schiller, S.; Singh, Y.; Viswam, S.; Bongs, K.; Häfner, S.; Herbers, S.; Dörscher, S.; Al-Masoudi, A.; et al. An Optical Lattice Clock Breadboard Demonstrator for the I-SOC Mission on the ISS. In Proceedings of the Lasers Electro-Optics Europe European Quantum Electronics Conference, Munich, Germany, 25–29 June 2017; p. 1.
4. Giorgetta, F.R.; Swann, W.C.; Sinclair, L.C.; Baumann, E.; Coddington, I.; Newbury, N.R. Optical two-way time and frequency transfer over free space. *Nat. Photonics* **2012**, *7*, 434–438. [[CrossRef](#)]
5. Deschênes, J.D.; Sinclair, L.C.; Giorgetta, F.R.; Swann, W.C.; Baumann, E.; Coddington, I.; Newbury, N.R. Synchronization of Optical Oscillators Over a Free-Space Link at the Femtosecond Level. In Proceedings of the Conference on Lasers and Electro-Optics (CLEO), San Jose, CA, USA, 10–15 May 2015.
6. Shen, Q.; Guan, J.Y.; Ren, J.G.; Zeng, T.; Hou, L.; Li, M.; Cao, Y.; Han, J.J.; Lian, M.Z.; Chen, Y.W.; et al. Free-space dissemination of time and frequency with 10^{−19} instability over 113 km. *Nature* **2022**, *610*, 661–666. [[CrossRef](#)] [[PubMed](#)]
7. Dix-Matthews, B.P.; Schediwy, S.W.; Gozzard, D.R.; Savalle, E.; Esnault, F.X.; Lévêque, T.; Gravestock, C.; D’Mello, D.; Karpathakis, S.; Tobar, M.; et al. Point-to-point stabilized optical frequency transfer with active optics. *Nat. Commun.* **2021**, *12*, 515. [[CrossRef](#)] [[PubMed](#)]
8. Leopardi, H.; Davila-Rodriguez, J.; Quinlan, F.; Olson, J.; Sherman, J.A.; Diddams, S.A.; Fortier, T.M. Single-branch Er:fiber frequency comb for precision optical metrology with 10^{−18} fractional instability. *Optica* **2017**, *4*, 879–885. [[CrossRef](#)]
9. Li, P.; Rolland, A.; Jiang, J.; Fermann, M.E. Coherent frequency transfer with < 5*10^{−21} stability via a multi-branch comb with noise cancellation. *Opt. Exp.* **2022**, *30*, 22957–22962.
10. Hećimović, Ž. Relativistic Effects on Satellite Navigation. *Tehnički Vjesnik/Technical Gazette.* **2013**, *20*, 195–203.
11. Meng, Z.; Guo, X.; Yang, J.; Yan, Q.; Zhang, Y.; Yang, F.; Wang, G.; Liu, K.; Chen, L.; Liu, Y.; et al. Method for Designing a Signal System for High-Precision Microwave Time-Frequency Transfer from Space to Ground. CN202110554869.0, 5 May 2023. Changsha Guoke Tianhe Intellectual Property Agency Co., Ltd. Available online: <https://d.wanfangdata.com.cn/patent/CN202310101879.8> (accessed on 12 July 2023).
12. Shen, W.; Zhang, P.; Shen, Z.; Xu, R.; Sun, X.; Ashry, M.; Ruby, A.; Xu, W.; Wu, K.; Wu, Y.; et al. Testing Gravitational Redshift Based on Microwave Frequency Links Onboard the China Space Station. *Phys. Rev. D* **2023**, *108*, 064031. [[CrossRef](#)]
13. Stone, W. *Two-Way Satellite Time and Frequency Transfer (TWSTFT): Principle, Implementation, and Current Performance*; Wiley-IEEE Press: Hoboken, NJ, USA, 2009.
14. Pan, J.Y.; Hu, X.G.; Tang, C.P.; Zhou, S.S.; Li, R.; Zhu, L.F.; Tang, G.F.; Hu, G.M.; Chang, Z.Q.; Wu, S.; et al. System error calibration for time division multiple access inter-satellite payload of new-generation Beidou satellites. *Chin. Sci. Bull.* **2017**, *62*, 2671–2679. [[CrossRef](#)]
15. Yang, Y.; Yang, Y.; Hu, X.; Tang, C.; Guo, R.; Zhou, S.; Xu, J.; Pan, J.; Su, M. BeiDou-3 broadcast clock estimation by integration of observations of regional tracking stations and inter-satellite links. *GPS Solut.* **2021**, *25*, 57. [[CrossRef](#)]
16. Zhang, S.; Gao, S.; Bai, Y.; Guo, Y.; Pan, Z.; Lu, X. A High-Precision Satellite-Ground Time Comparison Method and System Based on Tri-frequency Mode. CN202110554869.0. 21 May 2022. Available online: https://xueshu.baidu.com/usercenter/paper/show?paperid=1q5a0pc0x2630jh0ay0k0pq09g273141&site=xueshu_se (accessed on 24 July 2022).
17. Han, C.; Cai, Z. Relativistic effects to the onboard BeiDou satellite clocks. *Navigation* **2019**, *66*, 49–53. [[CrossRef](#)]
18. Sun, L.; Gao, Y.; Huang, W.; Li, P.; Zhou, Y.; Yang, J. Autonomous Time Synchronization Using BeiDou Inter-satellite Link Ranging. In Proceedings of the 2019 IEEE International Conference on Signal, Information and Data Processing (ICSIDP), Chongqing, China, 11–13 December 2019; pp. 1–5. [[CrossRef](#)]
19. Pan, J.; Hu, X.; Zhou, S.; Tang, C.; Guo, R.; Zhu, L.; Tang, G.; Hu, G. Time synchronization of new-generation BDS satellites using inter-satellite link measurements. *Adv. Space Res.* **2018**, *61*, 145–153. [[CrossRef](#)]

20. Sun, X.; Shen, W.B.; Shen, Z.; Cai, C.; Xu, W.; Zhang, P. Formulation to test gravitational redshift based on the tri-frequency combination of ACES frequency links. *Eur. Phys. J. C.* **2021**, *81*, 634. [[CrossRef](#)]
21. Delva, P.; Meynadier, F.; Le Poncin-Lafitte, C.; Laurent, P.; Wolf, P. Time and frequency transfer with a MicroWave Link in the ACES/PHARAO Mission. In Proceedings of the 2012 European Frequency and Time Forum, Gothenburg, Sweden, 23–27 April 2012; pp. 28–35.

Disclaimer/Publisher’s Note: The statements, opinions and data contained in all publications are solely those of the individual author(s) and contributor(s) and not of MDPI and/or the editor(s). MDPI and/or the editor(s) disclaim responsibility for any injury to people or property resulting from any ideas, methods, instructions or products referred to in the content.